

Accurate relative location using coda waves of a poorly recorded cluster of earthquakes near Kalannie, Western Australia

D. J. ROBINSON,^{1,2} M. SAMBRIDGE,¹ R. SNIEDER,³ P. CUMMINS^{1,2} AND J. DAWSON⁴

(Type abstract here)

1. Introduction

- South West Seismic Zone (SWSZ) - one of Australia's most active source zones
- Poor station coverage makes accurate location difficult
- Kalannie earthquake cluster (figure 1(a))
- *Dawson et al.* [2008] composite mechanism (ref table ??)
- Validity of composite mechanism assumes overlapping rupture on the same fault - we demonstrate that assumption holds despite the poor station coverage

2. Methodology

- Compute Kalannie event sizes (Table 1) and comment on location accuracy required to demonstrate that events are overlapping
 - Relative location with a few stations - use the coda
 - CWI separation (*Snieder and Vrijlandt*, 2005; *Snieder*, 2006)
 - Possible to get separation estimate with a single station (e.g. *Robinson et al.*, 2007)
 - ref **Paper1** - formulates CWI probabilistically for a pair of events - must comment on wavelength normalisation
 - ref **Paper2** - formulation of the joint posterior, misfit function L and minimization by optimisation.
- Problem with optimisation approach is that it gives a single solution only and can get trapped in local minima. We use Markov-Chain Monte-Carlo (MCMC) here which allows a complete assessment of uncertainty. This is only possible because of the small number of events considered.
- **Malcolm and Roel - there is potentially a large number of equations to show here. I propose that we keep the number of equations as small as possible and refer readers to the other papers and the thesis for details. Any thoughts?**

3. Results

- Discuss waveforms, first arrival similarity and filtering between 1 and 2 Hz (Figure 1(b))
- We only have access to data from 3 stations MORW, BLDU and KLBK (Figure 1(a))
 - Application of CWI on event pairs (Figure 1(b))
 - Computation of CWI based pairwise separation posteriors (Figure 2)
 - Compare MCMC results (Expected Value and standard error) to optimisation solution (Table 2)
 - MCMC in more detail: 1D marginals, covariance and correlation (Figure 3)
 - MCMC in more detail: example 2D marginal (Figure 4). Shows that events 1 and 2 are close but not co-located.
 - Discuss the separation estimates which incorporate CWI from all pairs (e.g. Table 3)

4. Conclusions

- The power of CWI when limited stations available
- Advantage of the MCMC inversion approach (i.e. detailed picture of uncertainty). Disadvantage that it is computationally expensive (ref **Paper2** for optimisation approach with more events).
- Demonstration that the events are close but not co-located. Consistent with hypothesis that the four ruptures overlap on the same fault.

Acknowledgments. (Text here)

References

- Clark, D. (2009), Identification of Quaternary scarps in southwest and central west Western Australia using DEM, *International Journal of Remote Sensing*, p. (submitted).
- Dawson, J., P. Cummins, P. Tregoning, and M. Leonard (2008), Shallow intraplate earthquakes in Western Australia observed by Interferometric Synthetic Aperture Radar, *Journal of Geophysical Research*, 113(B11408), doi:10.1029/2008JB005807.
- Robinson, D. J., M. Sambridge, and R. Snieder (2007), Constraints on coda wave interferometry estimates of source separation: The 2.5d acoustic case, *Exploration Geophysics*, 38(3), 189–199.
- Snieder, R. (2006), The theory of coda wave interferometry, *Pure and Applied Geophysics*, 163, 455–473.
- Snieder, R., and M. Vrijlandt (2005), Constraining the source separation with coda wave interferometry: Theory and application to earthquake doublets in the Hayward Fault, California, *Journal of Geophysical Research*, 110(B04301), doi:10.1029/2004JB003317.

D. J. Robinson, Research School of Earth Sciences, Australian National University, Canberra, ACT, 0200, Australia. (david.robinson@anu.edu.au) and Risk Research Group, Geoscience Australia, GPO Box 378, Canberra, ACT, 2601, Australia. (david.robinson@g.a.gov.au)

M. Sambridge, Research School of Earth Sciences, Australian National University, Canberra, ACT, 0200, Australia. (malcolm.sambridge@anu.edu.au)

R. Snieder, Center for Wave Phenomena and Department of Geophysics, Colorado School of Mines, Golden CO 80401, USA. (rsnieder@mines.edu)

P. Cummins, Research School of Earth Sciences, Australian National University, Canberra, ACT, 0200, Australia. (phil.cummins@anu.edu.au) and Risk Research Group, Geoscience Australia, GPO Box 378, Canberra, ACT, 2601, Australia. (phil.cummins@g.a.gov.au)

J. Dawson, Earth Monitoring Group, Geoscience Australia, GPO Box 378, Canberra, ACT, 2601, Australia. 1 (john.dawson@g.a.gov.au)

¹Research School of Earth Sciences, The Australian National University

²Risk Research Group, Geoscience Australia

³Center for Wave Phenomena and Department of Geophysics, Colorado School of Mines

⁴Earth Monitoring Group, Geoscience Australia

Copyright 2012 by the American Geophysical Union.
0094-8276/12/\$5.00

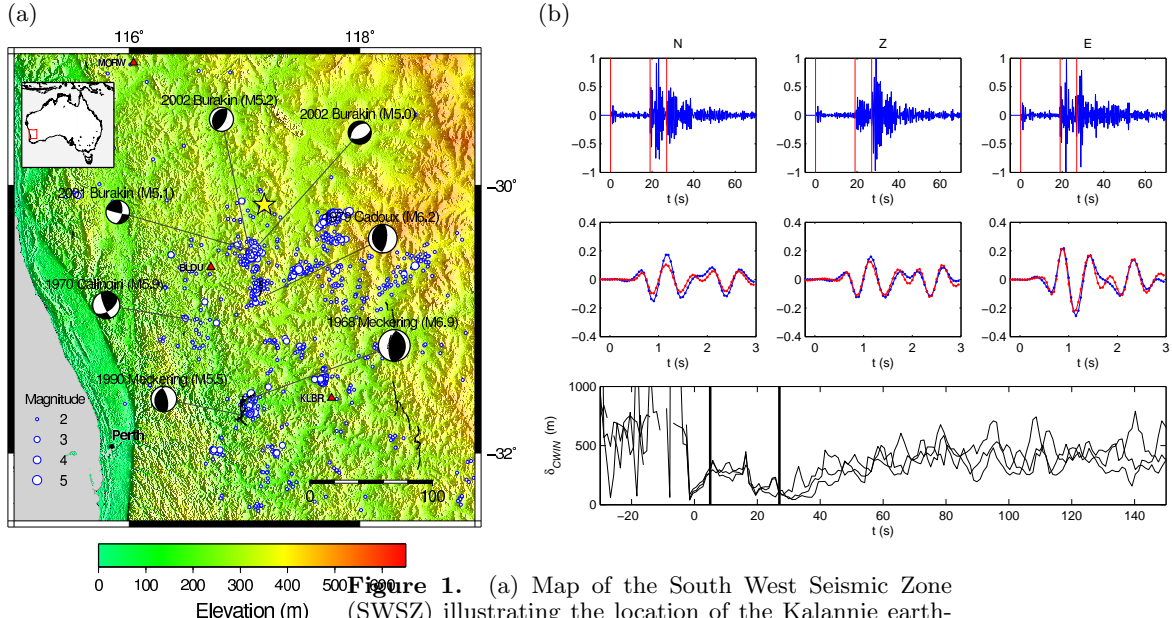


Figure 1. (a) Map of the South West Seismic Zone (SWSZ) illustrating the location of the Kalannie earthquake cluster, the *Dawson et al.* [2008] composite focal mechanism for the Kalannie events, large historical events (focal mechanisms), observed seismicity between 1998 to 2007 (circles) and Quaternary fault scarps (black lines) identified by *Clark* [2009]. The three available recording stations MORW (162 km), BLDU (67 km) and KLRB (169 km) are depicted with red triangles. Figure courtesy of *Dawson et al.* [2008] with minor modifications. (b) Example waveforms and CWI separation estimates for the Kalannie events. The top row illustrates waveforms at station MORW for Event 1 normalised to maximum amplitude and filtered between 1 and 2 Hz for the three channels N,Z,E. Relative P, S and surface wave arrivals are also indicated at 0, 19 and 27 s, respectively. Middle row demonstrates similarity of first arrivals at station MORW for Events 1 and 2 in the three channels. The bottom row shows the CWI separation estimates at MORW as a function of sliding time window with width 5 s for event pair 1 and 2. The three traces represent different channels and the vertical black lines enclose the region between $t = 5$ s and t_{surf} that we consider for the remaining analysis.

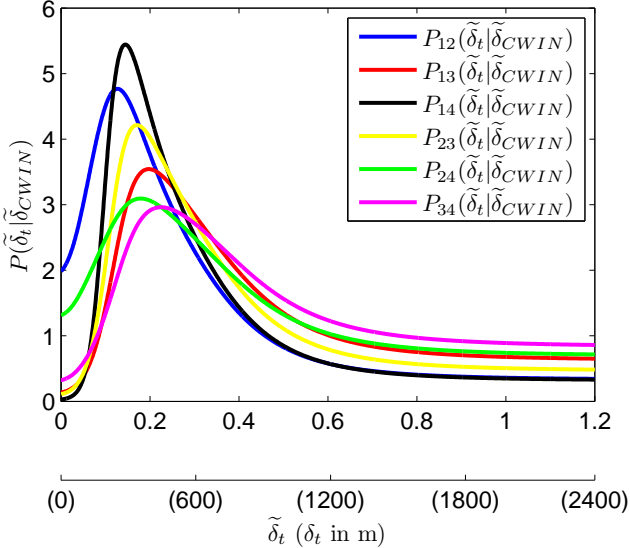


Figure 2. Posterior functions $P_{ij}(\tilde{\delta}_t|\tilde{\delta}_{CWIN})$ for the Kalannie event pairs i and j . A second x -axis is shown in separation units of meters for convenience.

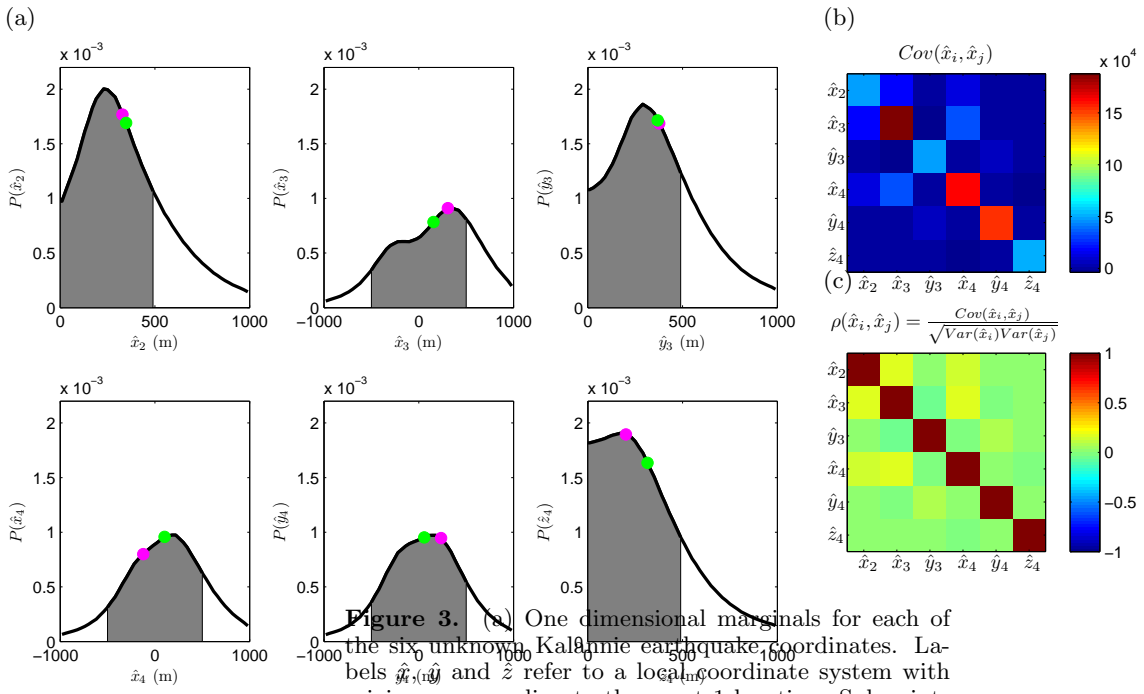


Figure 3. (a) One dimensional marginals for each of the six unknown Kalannie earthquake coordinates. Labels \hat{x} , \hat{y} and \hat{z} refer to a local coordinate system with origin corresponding to the event 1 location. Subscripts indicate the event number. Missing parameters \hat{y}_2 , \hat{z}_2 and \hat{z}_3 are set to 0 to remove rotational non-uniqueness without loss of generality. Grey shaded regions illustrate the probability of each coordinate being within 500 m of the origin. The relative size of the shaded area indicates that all event coordinates are likely within 500 m of event 1 (see table 2 for actual areas). (b) Covariance and (c) correlation matrices for the Kalannie earthquake location coordinates. Different colours in the covariance matrix suggest different levels of resolvability between coordinates. The off-diagonal structure of the correlation matrix indicates a low level of trade-off between different coordinates.

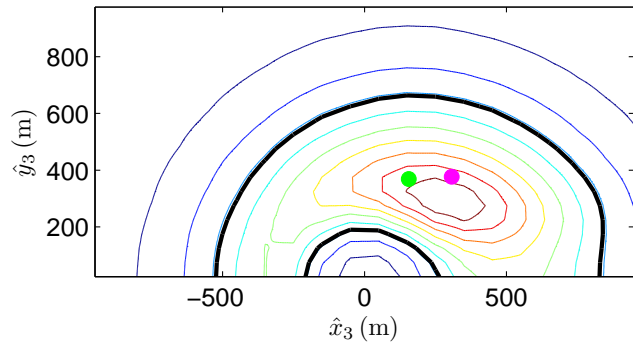


Figure 4. Marginal $P(\mathbf{e}_3) = P(\hat{x}_3, \hat{y}_3)$ for the location of event 3 normalised to unit volume. We observe a clear maximum near $(\hat{x}_3 = 290 \text{ m}, \hat{y}_3 = 300 \text{ m})$ and a local minimum near the origin. The black lines enclose the 68% confidence region. This figure suggests that events 3 and 1 (at origin) are close to one another but not co-located and is consistent with the inversion results from the optimiser (magenta circle) and MCMC (green circle).

Table 1. Estimated seismic moment M_o , moment magnitude M_w and rupture diameter $2a$ for the four Kalannie events using the local magnitude M_L of the Geoscience Australia catalogue and conversion formula discussed in text. In the case of the composite event (comp) we use the M_w of *Dawson et al. [2008]* and reverse the calculations.

Event	Date	M_L (2005)	M_o (10^{14} Nm)	M_w	$2a$ (m)
1	21-Sept	4	9.55	3.9	694
2	21-Sept	3.7	4.29	3.7	531
3	22-Sept	4.1	12.47	4	759
4	22-Sept	3.9	7.31	3.8	635
comp	NA	4.6	48.4	4.39	1192

Table 2. Inversion results for the Kalannie earthquake coordinates. The expected value $E[\bar{X}_i]$ and $var(\bar{X}_i)$ (the standard error of $E[\bar{X}_i]$) come from the Markov-chain Monte-Carlo approach, whereas \hat{x}_i^* result from the optimiser. The outputs of both inversion procedures are consistent within the bounds of the standard error. In the final column we show the probability of each event coordinate being within 500 m of the origin P_{500} (see grey shaded regions of figure 3)

parameter	$E[\bar{X}_i]$	$var(\bar{X}_i)$	\hat{x}_i^*	P_{500}
\hat{x}_2	348	220	329	0.76
\hat{x}_3	156	433	307	0.68
\hat{y}_3	369	223	377	0.73
\hat{x}_4	102	402	-124	0.76
\hat{y}_4	58	390	235	0.79
\hat{z}_4	315	224	201	0.81

Table 3. Separation estimates between Kalannie event pairs using the optimisation and Markov-chain Monte-Carlo (MCMC) inversion results. The separations are generally smaller than the anticipated rupture size of each event (see table 1) suggesting that the events could rupture overlapping sections of the same fault. We have more confidence in these separations than the pairwise CWI estimates because they simultaneously incorporate all coda wave data.

Pair	Optimiser	MCMC
δ_{12}	329	348
δ_{13}	486	401
δ_{14}	333	336
δ_{23}	378	416
δ_{24}	548	404
δ_{34}	496	446